Electronic Supplementary Information

Metallic CuNPs Confined Hollow Silicalite-1: Excellent Catalytic Efficiency of p-Nitrophenol Reduction

Rituparna Das, Sourav Ghosh and Milan Kanti Naskar

The role of TPAOH in the desilication process toward the formation of hollow silicalite-1

During the desilication process by TPAOH treatment, the surface Si–OH groups of crystals lose protons rendering negatively charged Si–O. These Si–O ions interact with TPA^+ ions, which reduce the dissolution of the external surface of silicalite-1. However, silicate oligomers are leached from the interior of the crystal, where crystallization is yet to be completed. The leached silicate oligomers interact with TPA^+ ions on the silicalite-1 surface forming a silicate/TPA intermediate state, and recrystallize at 170°C. Thus, continued desilication and recrystallization resulted in the formation of hollow silicalite-1 crystals.

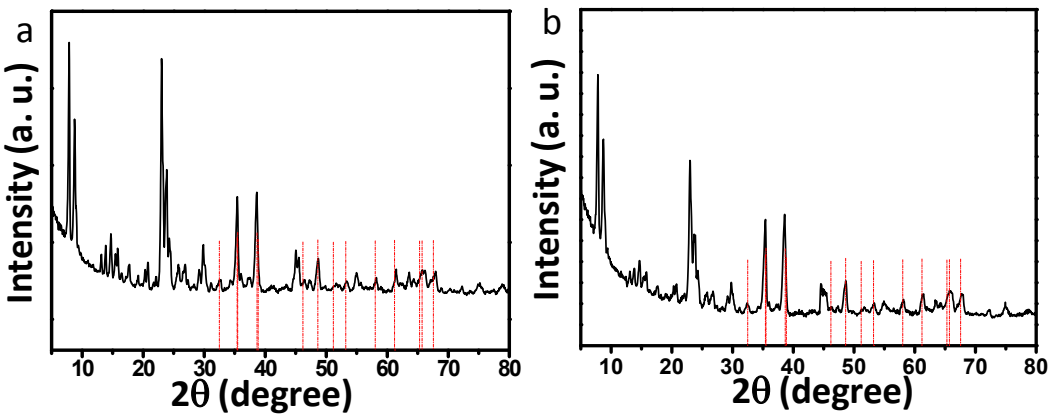

Fig. S1: XRD patterns of the calcined sample synthesized (a) before desilication (CuS-1) and (b) after desilication (CuHS-1) method .

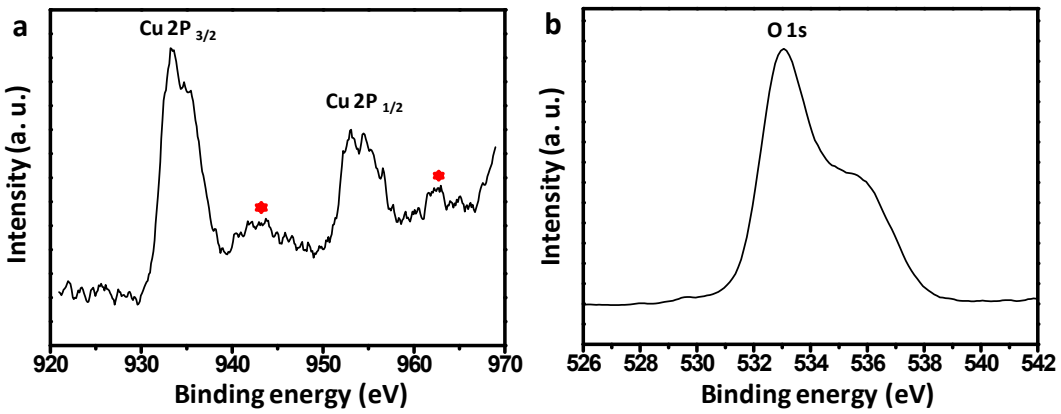

Fig. S2: (a) X-ray photoelectron spectra of 3d level of Cu and (c) 1s level of O present in CuS-1 (the star marks show the satellite peaks).

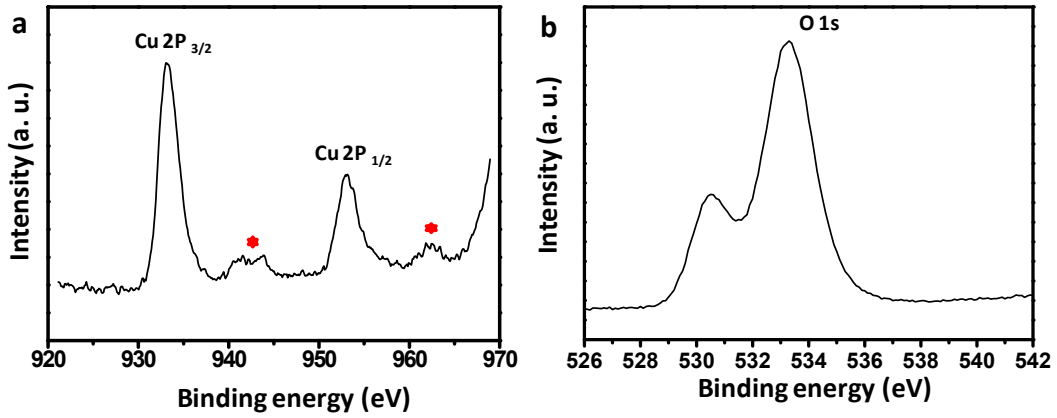

Fig. S3: (a) X-ray photoelectron spectra of 3d level of Cu and (c) 1s level of O present in CuHS-1 particles (the star marks show the satellite peaks).

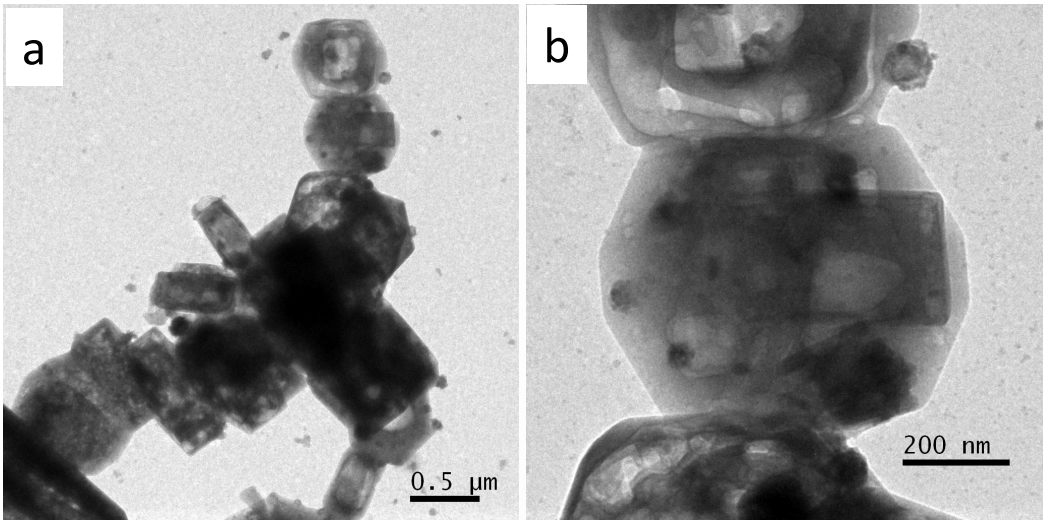

Fig. S4 : CuNPs were dispersed both in the exterior and interior surfaces of hollow silicalite-1

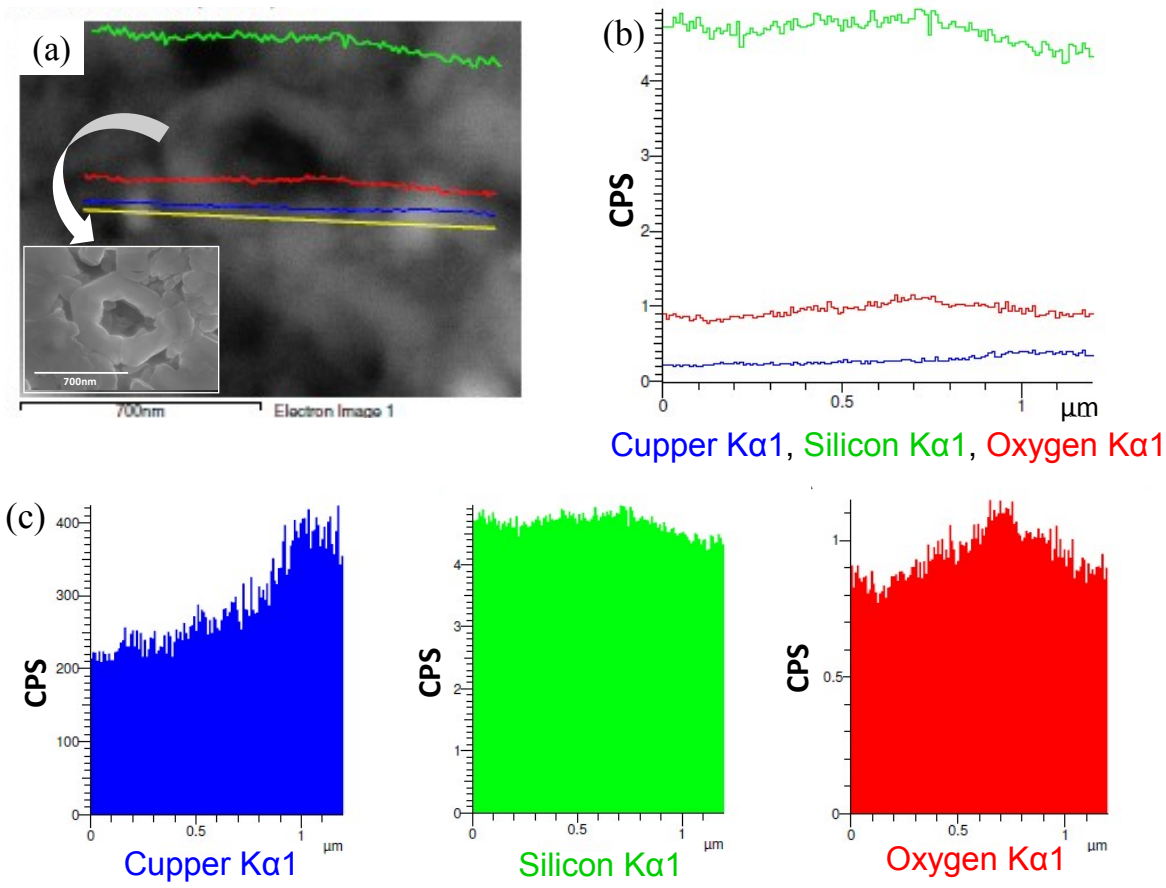

Fig. S5 : (a) Cross-sectional view of CuHS-1R along with back scatter electron image (inset shows secondary electron image), (b) depth concentration profile, and (c) line scan spectra of the elements Okα1, Si kα1 and Cukα1.

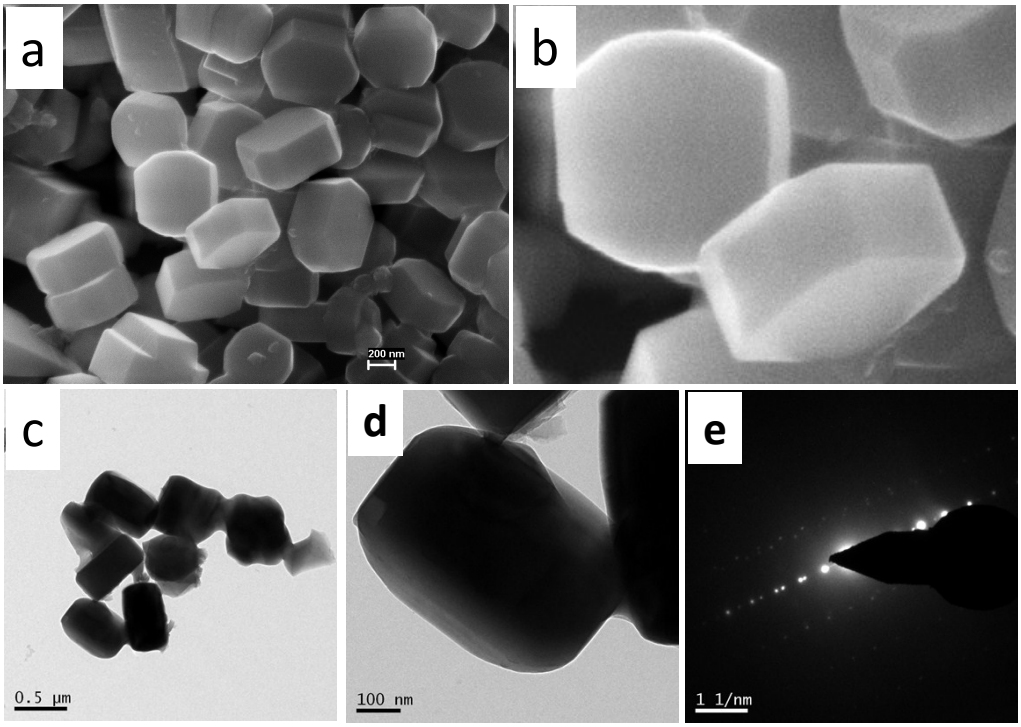

Fig. S6: (a, b) FESEM images, (c, d) TEM images and (e) SAED pattern of CuS-1 particles.

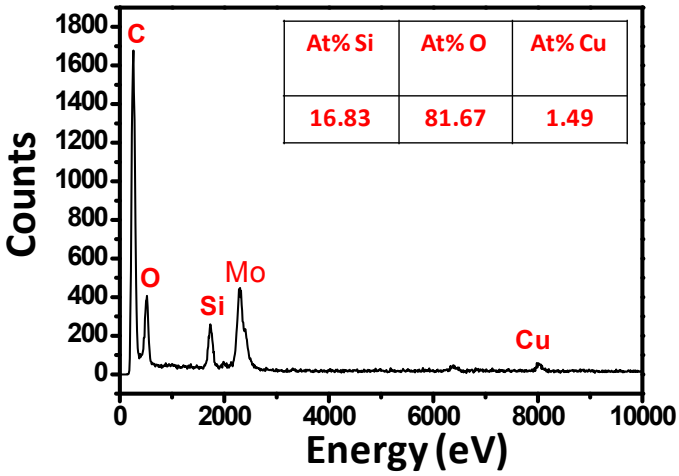

Fig. S7: EDS analysis of CuS-1 particles.

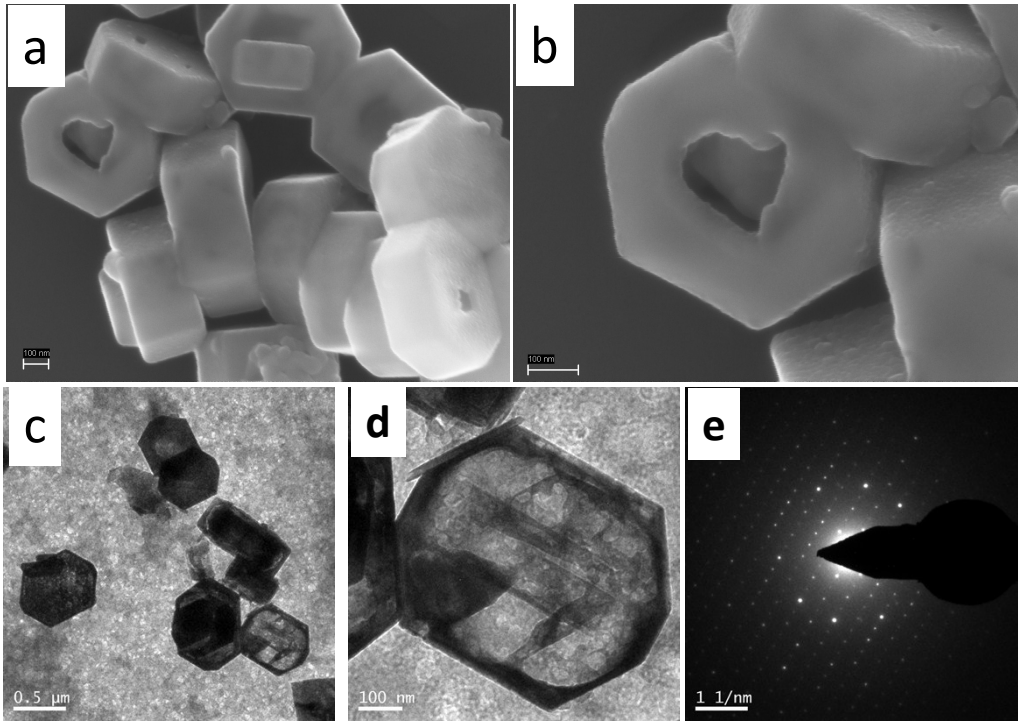

Fig. S8: (a, b) FESEM images, (c, d) TEM images and (e) SAED pattern of CuHS-1 particles.

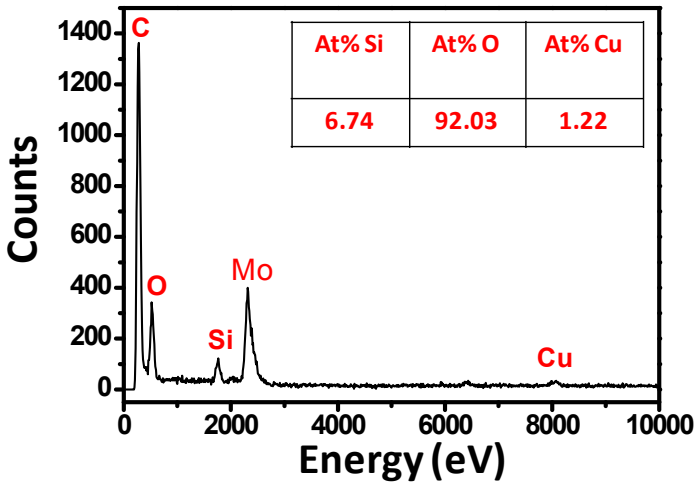

Fig. S9 : EDS analysis of CuHS-1 particles.

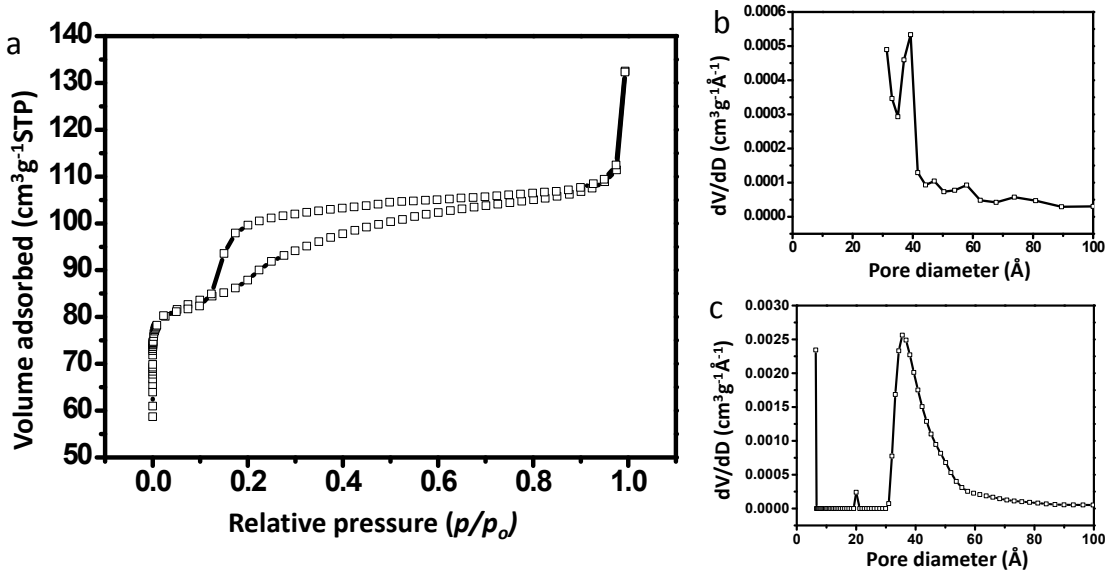

Fig. S10: (a) N_2 adsorption and desorption isotherms, pore size distributions (PSD) by (b) BJH and (c) DFT method of CuS-1 particles.

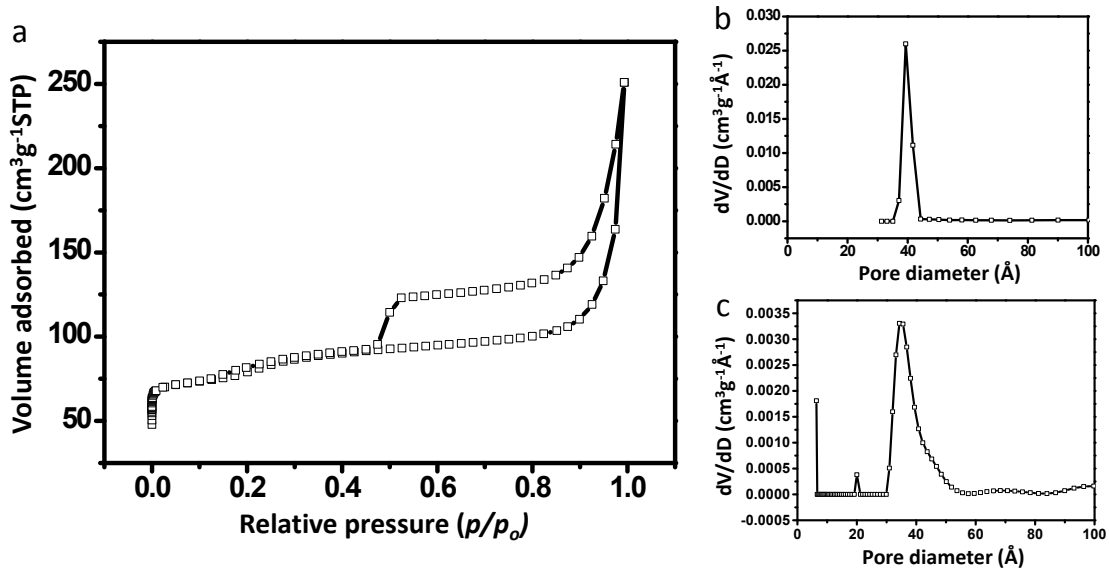

Fig. S11: (a) N_2 adsorption and desorption isotherms, pore size distributions (PSD) by (b) BJH and (c) DFT method of CuHS-1 particles.

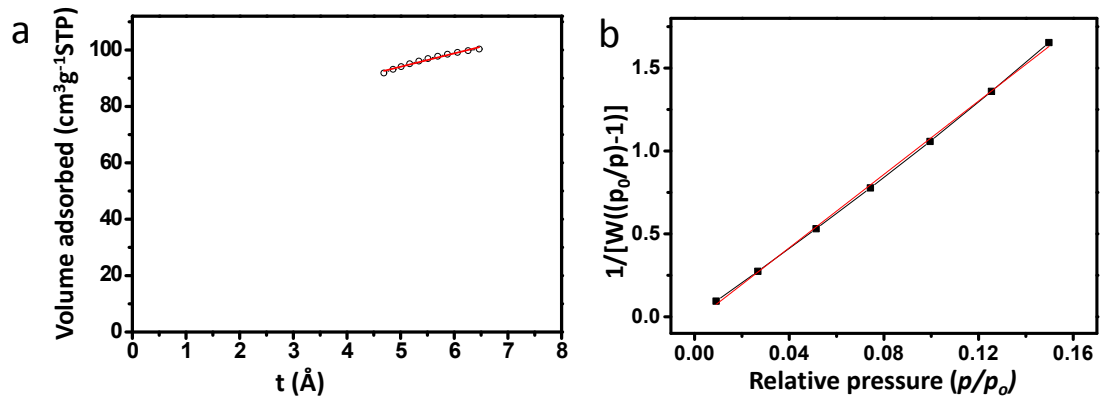

Fig. S12: (a) t-plot graph and (b) linear fitted plot of BET adsorption isotherm of CuS-1 particles. W is the weight of the gas adsorbed per gram of sample at relative pressure p/p_o.

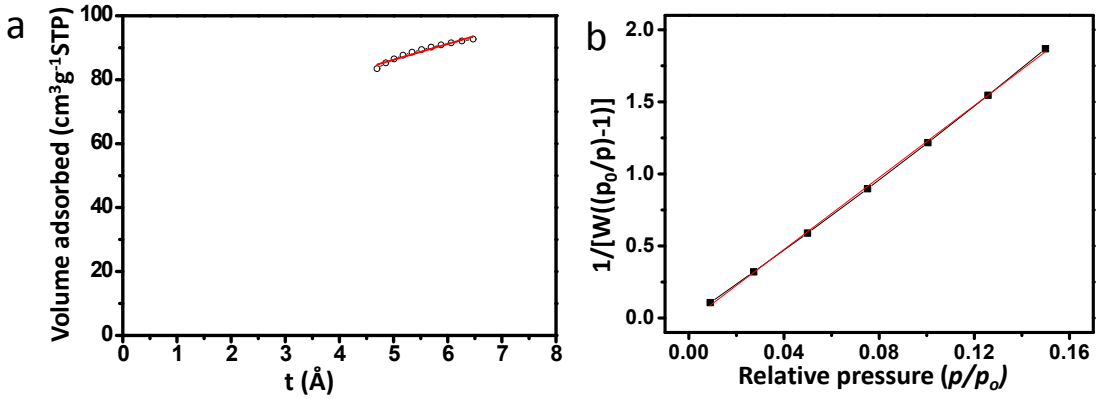

Fig. S13: (a) t-plot graph and (b) linear fitted plot of BET adsorption isotherm of CuHS-1 particles. W is the weight of the gas adsorbed per gram of sample at relative pressure p/p_o.

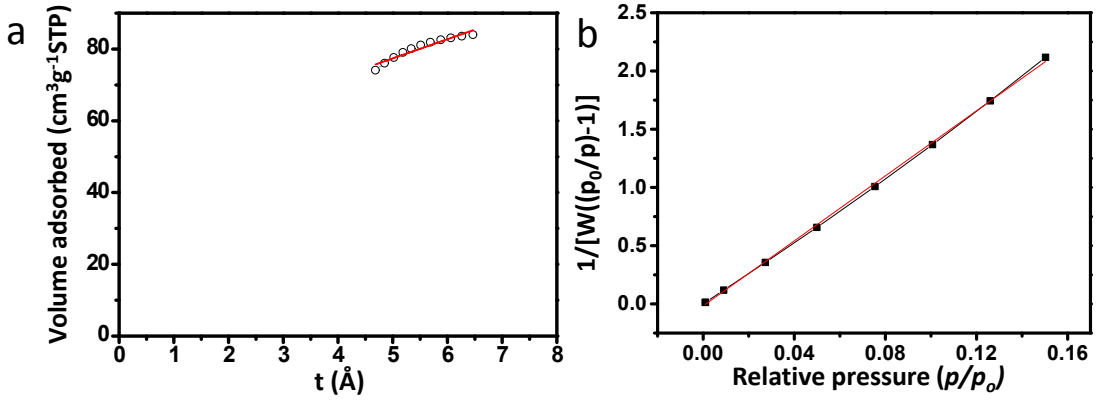

Fig. S14: (a) t-plot graph and (b) linear fitted plot of BET adsorption isotherm of CuHS-1R particles. W is the weight of the gas adsorbed per gram of sample at relative pressure p/p_o.

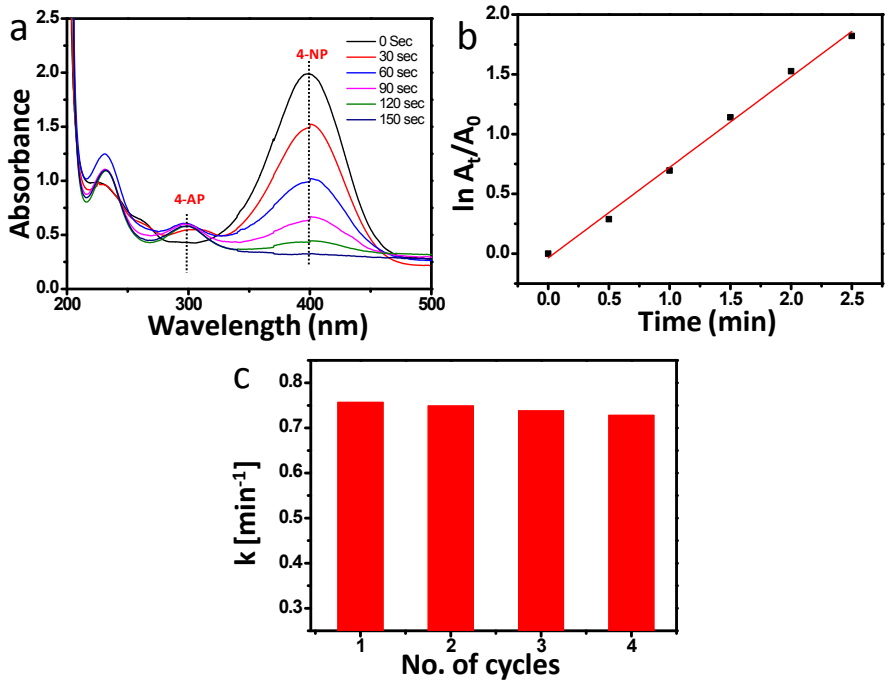

Fig.S15 : (a) Time dependent UV–visible absorption spectra for the reduction of p-nitro phenol in presence of 2 mg of CuNPs confined hollow silicalite-1 (CuHS-1R); (b) pseudo-first order plot of ($-\ln A_t/A_0$) versus reaction time for above reaction; (c) apparent rate constant values (k) for 4 consecutive cycles of the above catalytic reduction.

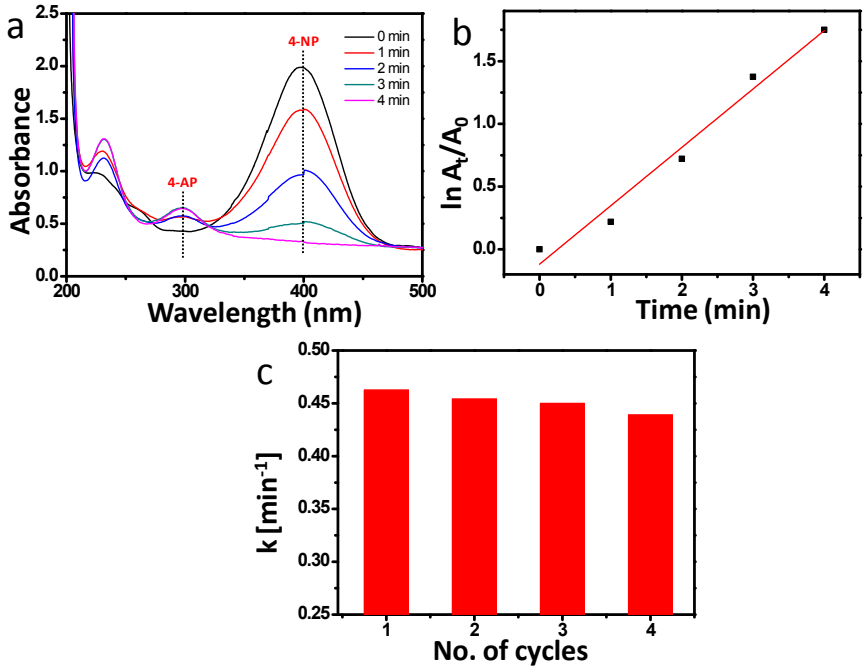

Fig.S16 : (a) Time dependent UV –visible absorption spectra for the reduction of p-nitro phenol in presence of 3 mg of CuNPs confined hollow silicalite-1 (CuHS-1R); (b) pseudo first order plot of ($-\ln A_t/A_0$) versus reaction time for above reaction; (c) apparent rate constant values (k) for 4 consecutive cycles of the above catalytic reduction.

Table S1: Comparison of apparent rate constant (k) and activity parameter (κ) of catalysts for PNP reduction.

Catalysts	(k) (s^{-1})	κ ($s^{-1}g^{-1}$)	References
CuNP aggregates	1.5x 10^{-3}	0.127	40
Spherical Ni	2.7x 10^{-3}	0.9	41
Coral like Ag-dendrite	5.1x 10^{-3}	1.29	44
[Au@Ag] MOF	4.9x 10^{-3}	1.43	45
Cu spheroid	1.8x 10^{-3}	1.88	5
CuNPs confined hollow silicalite-1 (CuHS-1R)	5.6x10^{-3}	44.09	This work

References:

44. M. H. Rashid and T. K. Mandal, *J. Phys. Chem. C*., 2007, **111**, 16750.
45. H.-L. Jiang, T. Akita, T. Ishida, M. Haruta and Q. Xu, *J. Am. Chem. Soc*., 2011, **133**, 1304.

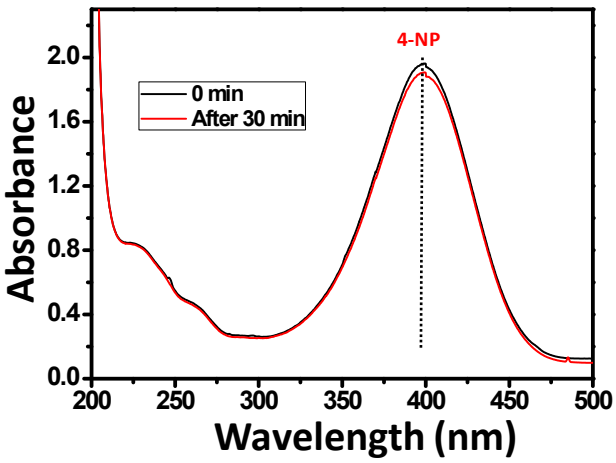

Fig.S17: UV–visible absorption spectra of the reduction of p-nitrophenol in the presence of 1 mg of pure silicalite-1 having no Cu species (S-1) at 0 min and after 30 min.

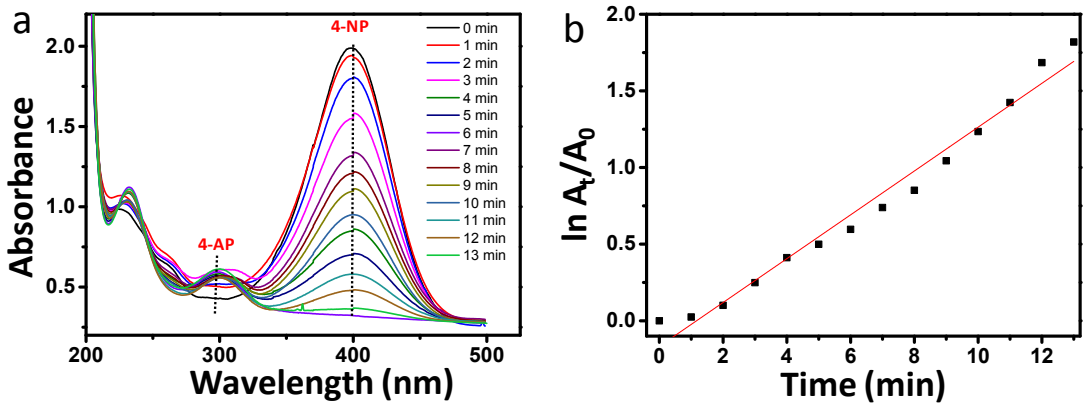

Fig.S18: (a) UV –visible absorption spectra of the reduction of p-nitrophenol in presence of 1mg CuS-1 particles; (b) pseudo first order plot of ($-\ln A_t/A_0$) versus reaction time for above reaction.

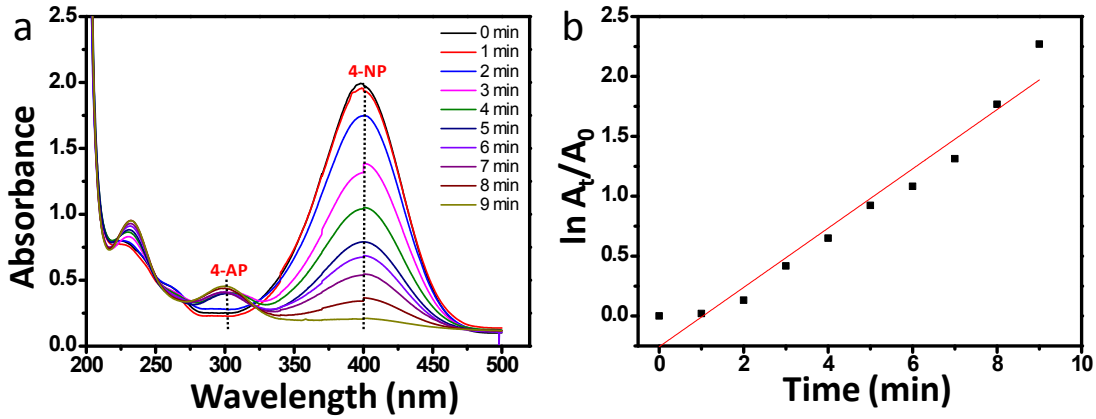

Fig.S19: (a) UV–visible absorption spectra of the reduction of p-nitrophenol in presence of 1 mg CuHS-1 particles; (b) pseudo-first order plot of ($-\ln A_t/A_0$) versus reaction time for the above reaction.

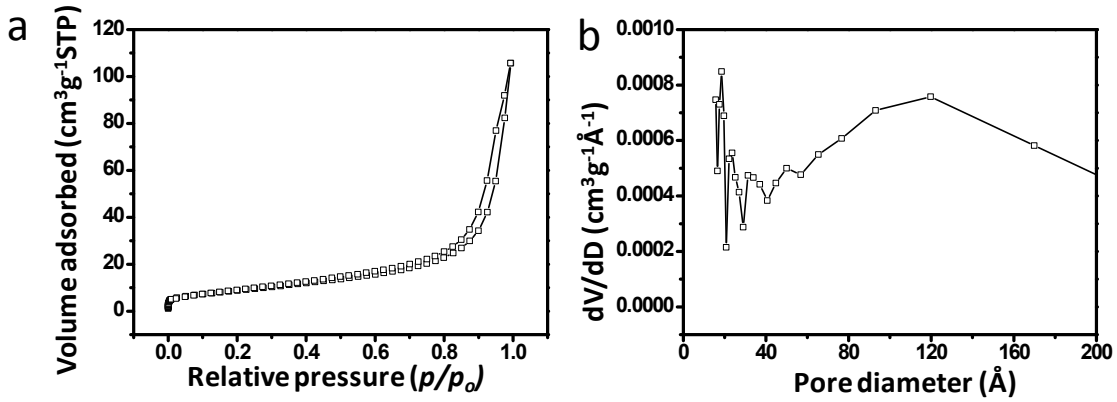

Fig. S20: (a) N_2 adsorption and desorption isotherms and (b) pore size distributions (PSD) by BJH method of CuNPs confined commercial 4A molecular sieve.

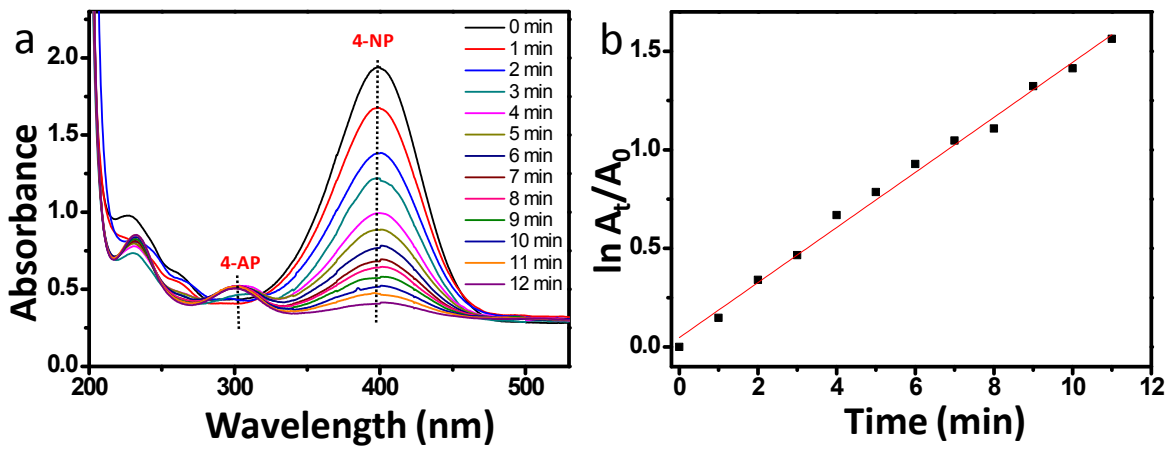

Fig.S21: (a) UV–visible absorption spectra of the reduction of p-nitrophenol in the presence of 1 mg of CuNPs confined commercial 4A molecular sieve; (b) pseudo-first order plot of ($-\ln A_t/A_0$) versus reaction time for the above reaction.